ROBUST MULTISCALE AM-FM DEMODULATION OF DIGITAL IMAGES

Víctor Murray[†]*, Paul Rodríguez V.*[‡] *and Marios S. Pattichis*[†]

[†]The University of New Mexico, Department of Electrical and Computer Engineering
Albuquerque, N.M. 87131, U.S.A.
Emails: vmurray@ieee.org, pattichis@ece.unm.edu
[‡]T-7, MS B284, Theoretical Division, Los Alamos National Laboratory,
Los Alamos, NM 87545, U.S.A.
Email: prodrig@istec.org

ABSTRACT

In this paper, we introduce new multiscale AM-FM demodulation algorithms that provide significant improvements in accuracy over previously reported approaches. The improvements are due to the use of new filterbanks based on separable filters supported in just two quadrants. The QEA, robust-QEA and Vakman methods are improved with this new filterbanks. A number of 2-D AM-FM examples are presented, where we observe significant accuracy improvements. For Lena, the mean-square-error for the AM-FM harmonic reconstruction is reduced by 88.31%. Similarly, for a AM-FM synthetic example of sinusoidal phase and Gaussian amplitude, the mean-square-error is reduced by: (i) 70.86% for the reconstruction, (ii) 99.66% for the instantaneous amplitude and (iii) 96.52% for the sinusoidal instantaneous frequency component.

Index Terms— Multidimensional demodulation, multidimensional amplitude modulation, multidimensional frequency modulation.

1. INTRODUCTION

Amplitude-modulation frequency-modulation (AM-FM) models allow us to model non-stationary image content in terms of a series expansion of AM-FM component images. We consider AM-FM expansions of the form:

$$I(x,\, y) = \sum_{n=1}^{n=M} a(x,\, y) \cos(n\, \varphi(x,\, y)). \tag{1}$$

In (1), an input image $I(.)$ is a function of a vector of spatial coordinates. A collection of M AM-FM harmonic images $a(x,\, y) \cos(\varphi(x,\, y))$ are used to reconstruct the input image. In this paper, we consider AM-FM components estimated over a multiscale filterbank (see Fig. 1).

The instantaneous amplitude (IA) functions $a(x,\, y)$ are always assumed to be positive. For each frequency modulated (FM) component, we associate an instantaneous frequency (IF) vector field $\nabla\varphi(x,\, y)$:

$$\nabla\varphi(x,\, y) = \left(\frac{\partial\varphi}{\partial x}(x,\, y),\, \frac{\partial\varphi}{\partial y}(x,\, y)\right). \tag{2}$$

Given a real image $I(x,\, y)$, we need to compute the AM-FM component images. We use the term AM-FM demodulation to imply the computation of the instantaneous amplitude (IA) $a(x,\, y)$, the phase function $\varphi(x,\, y)$, and the instantaneous frequency (IF) vector function $\nabla\varphi(x,\, y)$ from the given image $I(x,\, y)$. In this paper, we develop new multiscale filterbanks using separable 1D filters. With the new filterbanks, we were able to obtain significant improvements over our previously reported results [1]. In addition to image reconstruction methods, AM-FM models have been used in a variety of applications. Recently, theory and applications of multidimensional frequency modulation are reported in [2]. Prior applications include image retrieval in digital libraries [3] and video segmentation [4].

We summarize existing image demodulation methods in section 2. New filterbanks and the image reconstruction method are presented in section 3, and comparative results are shown in section 4. Concluding remarks are given in section 5.

2. AM-FM IMAGE DEMODULATION METHODS

2.1. Non-robust Demodulation

For any given image $f(.)$, we compute a two-dimensional analytic signal, as given in [5]:

$$f_{AS}(x,\, y) = f(x,\, y) + j\mathcal{H}_{2d}[f(x,\, y)], \tag{3}$$

where $\mathcal{H}_{2d}$ denotes the one-dimensional Hilbert transform operator applied along the rows (or columns). We estimate the instantaneous amplitude, the instantaneous phase, and the in-

stantaneous frequency using

$$a(x,\, y) = |f_{AS}(x,\, y)|, \tag{4}$$

$$\varphi(x,\, y) = \arctan\left(\frac{\text{imag}(f_{AS}(x,\, y))}{\text{real}(f_{AS}(x,\, y))}\right) \quad \text{and} \tag{5}$$

$$\omega(x,\, y) = \text{real}\left[-j\frac{\nabla f_{AS}(x,\, y)}{f_{AS}(x,\, y)}\right]. \tag{6}$$

The algorithm can be summarized into two steps. First, we compute the analytic signal using (3). Second, we compute all the estimates using (4), (5), (6). A discrete-space extension of the algorithm can be developed using the quasi eigenfunction approximation [6]. This leads to the following discrete formulas for estimating the instantaneous frequency vectors:

$$\frac{\partial\varphi}{\partial x}(k_1,\, k_2) \approx \arcsin\left[\frac{f_{AS}(k_1+1,\, k_2) - f_{AS}(k_1-1,\, k_2)}{2jf_{AS}(k_1,\, k_2)}\right], \tag{7}$$

$$\frac{\partial\varphi}{\partial y}(k_1,\, k_2) \approx \arcsin\left[\frac{f_{AS}(k_1,\, k_2+1) - f_{AS}(k_1,\, k_2-1)}{2jf_{AS}(k_1,\, k_2)}\right], \tag{8}$$

$$\frac{\partial\varphi}{\partial x}(k_1,\, k_2) \approx \arccos\left[\frac{f_{AS}(k_1+1,\, k_2) + f_{AS}(k_1-1,\, k_2)}{2f_{AS}(k_1,\, k_2)}\right], \tag{9}$$

$$\frac{\partial\varphi}{\partial y}(k_1,\, k_2) \approx \arccos\left[\frac{f_{AS}(k_1,\, k_2+1) + f_{AS}(k_1,\, k_2-1)}{2f_{AS}(k_1,\, k_2)}\right]. \tag{10}$$

2.2. Robust Demodulation Using the Quasi-Eigenfunction Approximation

It can be shown that the quasi-eigenfunction approximation described in (7)-(10) is numerically unstable. To show this, in [1] we computed the condition numbers of each one of the inverse trigonometric functions, and noted that they can grow unbounded at different frequencies (also see [7] for the definition of the condition number). However, it turns out that the functions are unbounded over different, discrete fourier frequencies. Thus, a robust demodulation algorithm can be designed that chooses between (7) and (9) and also between (8) and (10) for estimating the components of the instantaneous-frequency. Dramatic improvements are possible using this approach [1].

2.3. Continuous-Space, Multidimensional Demodulation for the Quasi-Local Method

We first assume that the input image is a single AM-FM harmonic $f(x,\, y) = a(x,\, y)\, \cos\varphi(x,\, y)$. For estimating the IA, we first noted that

$$2f^2(x,y) = a^2(x,y) + a^2(x,y)\cos(2\varphi(x,y)). \tag{11}$$

If we use a lowpass filter $h(.)$ to reject the high frequencies in (11), we get the IA estimate [1]

$$\hat{a}(x,y) = \sqrt{2f^2(x,y) * h(x,y)}. \tag{12}$$

Define g_x by

$$g_x(\epsilon_1,\epsilon_2) = f(x+\epsilon_1, y)f(x-\epsilon_2, y) \tag{13}$$

and R_x by

$$R_x(\epsilon) = \frac{2h(x,\, y) * \{g_x(\epsilon,\epsilon)\}}{h(x,\, y) * \{g_x(\epsilon,0) + g_x(0,\epsilon)\}} \tag{14}$$

Then, using R_x, we can get an IF estimate along the x-component using (see [1])

$$\left|\frac{\partial\varphi(x,\, y)}{\partial x}\right| = \lim_{\epsilon\to 0^+}\left\{\frac{1}{\epsilon}\arccos\left(\frac{R_x(\epsilon) + \sqrt{R_x^2(\epsilon)+8}}{4}\right)\right\}.$$

The discrete-space algorithm follows directly by considering a discrete lattice for $x,\, y$, so that $(x,\, y) = (n\Delta x,\, m\Delta y)$, for $n,\, m \in \mathbb{Z}$ and for ϵ to be some positive integral multiple of Δx. For the y-dimension, a similar approach can be taken. Furthermore, it is straight-forward how to extend the algorithm for any finite number of dimensions.

To estimate the signs of the IF vector components, we use a hybrid approach that uses (6) to determine the sign. Furthermore, in the hybrid approach, we use (5) for estimating the phase.

3. NEW FILTERBANKS AND RECONSTRUCTION

In this paper, we consider multiscale, separable approximations for implementing the demodulation filterbanks.
For estimating the correct 2D frequency, each filter has frequency support in just two quadrants (Fig. 1 (a), (b) and, (c)). This leads to better estimates than estimates from the use of Wavelet-type filters supported in all four quadrants. Also, with the coverage of the full 2D frequency spectrum, the proposed use of multiscale filterbanks leads to much better frequency-domain localization of the instantaneous frequency.
Each filter was designed to have a pass band ripple of 0.001dB and a stop band ripple of 0.0005dB. For the design, we used equiripple dyadic FIR filters. We designed filterbanks using two, three and four levels (see Fig. 1 (a)-(c)).
We consider reconstructing an image using M AM-FM harmonics:

$$\hat{I}(x,y) = \sum_{n=1}^{n=M} c_n a(x,y)\cos\left(n\varphi(x,y)\right). \tag{15}$$

Then, we want to compute the AM-FM harmonic coefficients $c_n,\, n = 1,2,\ldots,M$, so that $\hat{I}(x,y)$ is a least-squares estimate of $I(x,y)$ over the space of the AM-FM harmonics.

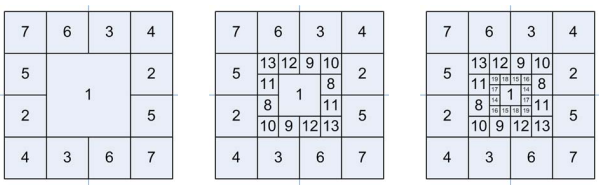

(a) (b) (c)

Fig. 1. New multiscale filterbanks with filters supported in just two quadrants: (a) Seven filters, (b) Thirteen filters, and (c) Nineteen filters.

We compute c_n using:

$$\begin{bmatrix} c_1 \\ \vdots \\ c_h \end{bmatrix} = \left(A^T A\right)^{-1} \left(A^T b\right), \tag{16}$$

where the columns of A are the AM-FM harmonics, and b is a column vector of the input image. We also compute an orthonormal basis over the space of the AM-FM harmonics using the Modified Gram-Schmidt (MGS) Algorithm [8]).

4. RESULTS

We present comparative results from demodulation from a real-life example (Lena) and a synthetic image. All the reconstructions were computed using ten AM-FM harmonics. In both cases, 512x512 gray images were used. Fig. 2 shows the values of the mean-square-error (MSE) for the reconstruction of the images, while Table 1 shows the improvement, in percentage, in terms of MSE of the new filterbanks compared with previous approaches (see [1]). With the use of just one harmonic, a reduction up to 88.31% of the original MSE was reached in the case of Lena, and up to 70.86% in the case of the synthetic data. We can see how increasing the number of harmonics used for the reconstruction, we get lower MSE values. From the results, Fig. 2 shows how the robust QEA method always produces the best results (lowest MSE).
Fig. 3 shows results related to Lena. The original image is shown in (a) whereas the reconstruction using the robust QEA method is shown in (c). With the use of the new filterbank, the reconstruction was improved up to 71.02 of MSE (85.04% of reduction compared with [1]) in (d). The estimation of the phase without considering the low frequencies is shown in (b). This result shows how the new filterbank, together with the robust QEA method, is able to track the high frequency changes in Lena's hair (Fig. 3 (e) and (f)).
In the case of the synthetic example (Fig. 4(a)), it was generated using:

$$I(x,\, y) = e^{\left(-\left(\frac{2x}{N}\right)^2 - \left(\frac{2y}{N}\right)^2\right)} \cos\left(2\pi\left(0.1y + \cos\left(0.1x\right)\right)\right), \tag{17}$$

	MSE value				
	Number of harmonics				
	1	2	4	6	10
Lena rec.	72.21	71.66	71.45	71.40	71.02
syn. im. rec	0.02	0.02	0.02	0.02	0.02
	Reduction in MSE (%)				
	1	2	4	6	10
Lena rec.	88.31	88.25	86.28	86.09	85.04
syn. im. rec.	70.86	70.86	64.99	64.95	64.81
syn. im. IA	99.662				
syn. im. IFx	96.524				
syn. im. IFy	98.724				

Table 1. Performance in the reconstruction of the images in terms of the MSE, and performance in the reduction of the MSE for the reconstruction, IA and IF estimations compared with [1].

for $x,\, y = -\frac{N}{2}, \ldots, \frac{N}{2} - 1$. The original image (Fig. 4(a)) and the original IA (b) are compared. The IA estimated using [1] is shown in (d) and it is clearly of lower quality as compared to the IA estimated with the new filterbank (f). The new reconstruction (e) has lower MSE than the one in (c). The reduction of the MSE in [1] was up to 70.86% for the reconstruction and up to 99.662% for the IA.

5. CONCLUSIONS

With the improved reconstruction of the images, a wide range of applications can benefit. Moreover, high-frequency changes in real-life images can now be successfully tracked (as demonstrated in the case of Lena's hair). Clearly, all prior applications that were based on AM-FM demodulation can benefit from using the new filterbanks presented in this paper.

6. REFERENCES

[1] P. Rodriguez V. and M.S. Pattichis, "New algorithms for fast and accurate am-fm demodulation of digital images," in *IEEE International Conference on Image Processing*, 2005.

[2] Marios S. Pattichis and Alan C. Bovik, "Analyzing image structure by multidimensional frequency modulation," *IEEE Transactions on Pattern Analysis and Machine Intelligence*, vol. 29, no. 5, pp. 753–766, 2007.

[3] J.P. Havlicek, J. Tang, S.T. Acton, R. Antonucci, and F.N. Quandji, "Modulation domain texture retrieval for cbir in digital libraries," in *Proc. 37th IEEE Asilomar Conf Signals, Syst., Comput.*, Pacific Grove, CA, november 2003.

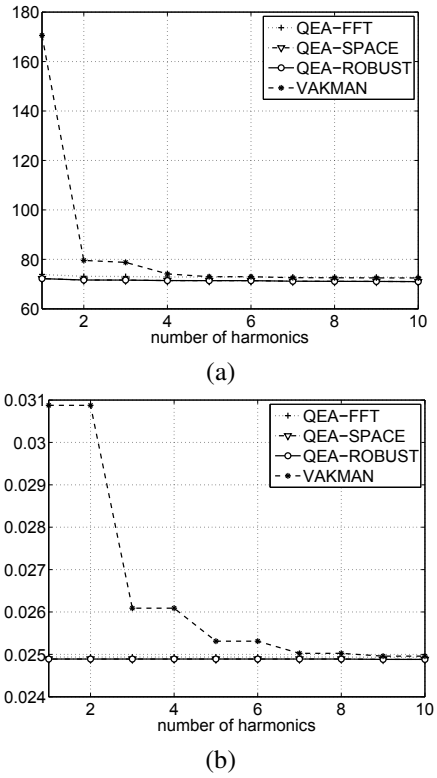

Fig. 2. MSE in the reconstruction using the robust QEA. (a) Lena. (b) Synthetic image.

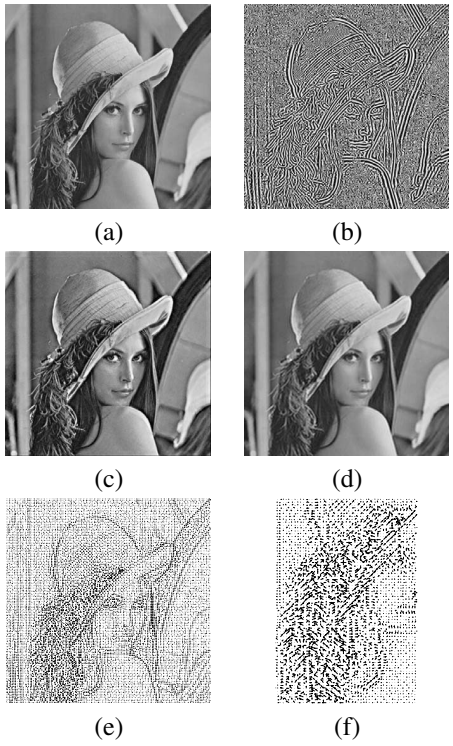

Fig. 3. Results for Lena using three levels in the filterbank. (a) Original image, (b) $\cos\varphi(x,y)$ without the use of the LPF, (c) Image reconstruction using the robust QEA method in [1], (d) Image reconstruction using the robust QEA method with new filterbanks, (e) IF vectors and, (f) Zoom of the IF to *Lena*'s hair.

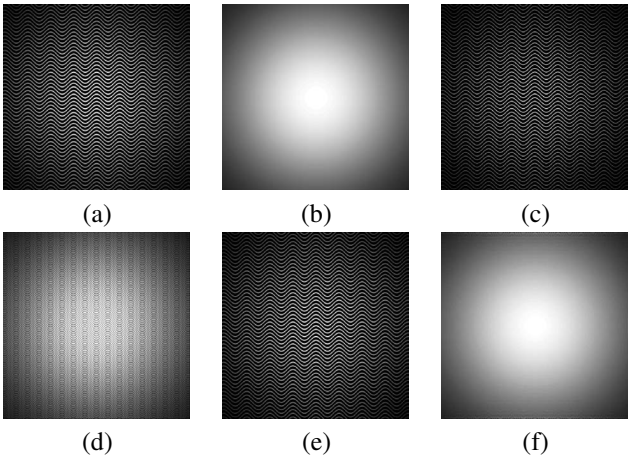

Fig. 4. Results for synthetic image using two levels in the filterbank. (a) Original image, (b) Original IA, (c) Image reconstruction using the robust QEA method in [1], (d) IA using the robust QEA method in [1], (e) Image reconstruction using the robust QEA method with new filterbanks, (f) IA using the robust QEA method with new filterbanks.

[4] P. Rodriguez V., M.S. Pattichis, and M.B. Goens, "M-mode echocardiography image and video segmentation based on am-fm demodulation techniques," in *Proc. of the 25th Intern. Conf. of the IEEE Engineering in Medicine and Biology Society (EMBS 2003)*, september 2003, vol. 2, pp. 1176–1179.

[5] J. P. Havlicek, *AM-FM Image Models*, Ph.D. thesis, The University of Texas at Austin, 1996.

[6] Joseph P. Havlicek, David S. Harding, and Alan Conrad Bovik, "Multidimensional quasi-eigenfunction approximations and multicomponent AM-FM models," *IEEE Transactions on Image Processing*, vol. 9, no. 2, pp. 227–242, february 2000.

[7] Samuel D. Conte and Carl de Boor, *Elementary Numerical Analysis: An Algorithmic Approach*, McGrawHill, 1980.

[8] James W. Demmel, *Applied Numerical Linear Algebra*, chapter Linear Least Square Problems, pp. 105–117, SIAM, 1997.